A structure-based site-directed mutagenesis study on the neurolysin (EC 3.4.24.16) and thimet oligopeptidase (EC 3.4.24.15) catalysis

Vitor Oliveira[a,*], Maurício C. Araújo[b], Vanessa Rioli[b], Antonio C.M. de Camargo[c], Ivarne L.S. Tersariol[d], Maria A. Juliano[a], Luiz Juliano[a], Emer S. Ferro[b]

[a] *Departamento de Biofísica, Universidade Federal de São Paulo, 04044-020 São Paulo, SP, Brazil*
[b] *Departamento de Histologia e Embriologia, Programa de Biologia Celular, Instituto de Ciências Biomédicas, Universidade de São Paulo, 05508-900 São Paulo, SP, Brazil*
[c] *Centro de Toxinologia Aplicada (CAT), Instituto Butantan, 05467-010 São Paulo, SP, Brazil*
[d] *Centro Interdisciplinar de Investigação Bioquímica (CIIB), Universidade de Mogi das Cruzes, 08780-911 Mogi das Cruzes, SP, Brazil*

Received 10 February 2003; revised 18 March 2003; accepted 18 March 2003

First published online 1 April 2003

Edited by Hans-Dieter Klenk

Abstract Neurolysin (EP24.16) and thimet oligopeptidase (EP24.15) are closely related metalloendopeptidases. Site-directed mutagenesis of Tyr^{613} (EP24.16) or Tyr^{612} (EP24.15) to either Phe or Ala promoted a strong reduction of k_{cat}/K_M for both enzymes. These data suggest the importance of both hydroxyl group and aromatic ring at this specific position during substrate hydrolysis by these peptidases. Furthermore, the EP24.15 A607G mutant showed a k_{cat}/K_M of 2×10^5 M^{-1} s^{-1} for the Abz-GFSIFRQ-EDDnp substrate, similar to that of EP24.16 ($k_{cat}/K_M = 3\times10^5$ M^{-1} s^{-1}) which contains Gly at the corresponding position; the wild type EP24.15 has a k_{cat}/K_M of 2.5×10^4 M^{-1} s^{-1} for this substrate.

Key words: Enzyme specificity; Catalytic mechanism; Site-directed mutagenesis

1. Introduction

Neurolysin (EC 3.4.24.16; EP24.16) and thimet oligopeptidase (EC 3.4.24.15; EP24.15) were initially detected in and purified from rat brain homogenates [1,2]. EP24.15 and EP24.16 are zinc-dependent peptidases, members of the metallopeptidase M3 family, containing in the primary sequence the HEXXH motif [3,4]. In the 3D structure of EP24.16 the catalytic center is located in a deep channel, which limits the access to only short peptides [5,6]. This selectivity for oligopeptides as substrates was also verified for EP24.15 [6–8]. Moreover, the high primary sequence identity found for these related peptidases, which are up to 65% identical [4], allows the assumption that these enzyme also share the same pattern of folding [9].

Detailed analyses of substrate specificity for EP24.16 and EP24.15 have been reported using internally quenched fluorogenic peptides derived from bradykinin [6] or neurotensin [10]. An outstanding feature of the hydrolytic activities of EP24.16 and EP24.15 on these substrates was the variability of the cleavage sites [6]. This behavior was interpreted as the ability of the substrates to bind at different subsites in the catalytic center [6]. The 3D structure determination of EP24.16 supports the view of a broad specificity for these enzymes [9], suggesting the possibility of a reorganization of flexible loops in the enzyme peptide binding site to accommodate the substrates [5,9]. Furthermore, an overview of the EP24.16 crystal structure revealed that the phenolic group of the Tyr^{613} residue[1] is facing the metal ion from the catalytic center [5]. Similarly, an EP24.15 structure-based model suggested that the corresponding Tyr^{612} residue is also positioned close to the catalytic center zinc ion [9].

In the present work we report the mutation of this Tyr residue positioned close to the active center to either Phe or Ala, on both EP24.16 and EP24.15. Our data suggest that both the hydroxyl group and the aromatic ring of this specific Tyr residue are important for substrate catalysis by these peptidases. In addition, we have demonstrated that Ala^{607} is an important residue to drive the substrate specificity of EP24.15, directly interacting with the substrate and/or changing the flexibility of the loop which is in position to interact with the P1 residue from the substrate [5,9].

2. Materials and methods

2.1. Site-directed mutagenesis and protein expression

The QuikChange site-directed mutagenesis kit (Stratagene, La Jolla, CA, USA) was used to introduce specific point mutations in the wild type EP24.15 or EP24.16 cDNA, as previously described [11]. Point mutations were specified as Y612F, Y612A and A607G for EP24.15, and Y613F and Y613A for EP24.16. Expression and purification of the wild type or mutant proteins for biochemical characterization were done in *Escherichia coli*, using the pGEX4T-2 plasmid (Amersham Pharmacia Biotech), as previously described [12], with all enzymes stored at −80°C for subsequent analysis.

2.2. Enzyme activity assay and determination of kinetic parameters

The kinetic parameters for hydrolysis of the substrates were deter-

*Corresponding author. Present address: Centro Interdisciplinar de Investigação Bioquímica, Sala 1S-15, Av. Dr. Candido Xavier de Almeida Souza 200, CEP 08780-911, Mogi das Cruzes, SP, Brazil. Fax: (55)-11-4798 7068.
E-mail address: vitor.biof@infar.epm.br (V. Oliveira).

Abbreviations: Abz, *ortho*-aminobenzoic acid; EDDnp, *N*-(2,4-dinitrophenyl) ethylenediamine

[1] We are using the numbers as used in the rat neurolysin structure description and the corresponding residue to this Tyr^{613} in the alignment of all M3 family member sequences in the MEROPS database is Tyr^{611} [23].

0014-5793/03/$22.00
doi:10.1016/S0014-5793(03)00310-7

mined by initial rate measurements. The hydrolysis of the fluorogenic substrates was done at 37°C in 50 mM Tris–HCl buffer pH 7.4 containing 100 mM NaCl and followed by measuring the fluorescence at $\lambda_{em} = 420$ nm and $\lambda_{ex} = 320$ nm in a Hitachi F-2000 spectrofluorometer. The 1 cm path length cuvette containing 2 ml of the substrate solution was placed in a thermostatically controlled cell compartment for 5 min before the enzyme solution was added (for EP24.15 an additional preincubation time of 5 min with 0.5 mM of dithiothreitol was applied after enzyme addition) and the increase in fluorescence with time was continuously recorded for 5–10 min. The slope was converted into mol hydrolyzed substrate per minute based on the fluorescence curves of standard peptide solutions before and after total enzymatic hydrolysis. The concentration of the peptide solutions was obtained by colorimetric determination of the 2,4-dinitrophenyl group (17 300 M^{-1} cm^{-1}, extinction coefficient at 365 nm). The enzyme concentration for initial rate determination was chosen at a level to hydrolyze less than 5% of the substrate present. The inner filter effect was corrected using an empirical equation as previously described [13]. The kinetic parameters were calculated according Wilkinson [14], as well as by using Eadie–Hofstee plots. All the obtained data were fitted to non-linear least square equations, using Grafit v. 3.0 from Erithacus Software.

2.3. Determination of cleaved bonds

The cleaved bonds were identified by isolation of the fragments by high performance liquid chromatography and the retention times of the products fragments were compared with authentic synthetic sequences and/or by molecular weight, which was determined by matrix assisted laser desorption ionization/time of flight mass spectrometry and/or by peptide sequencing, using a protein sequencer PPSQ-23 (Shimadzu Tokyo, Japan).

2.4. Circular dichroism (CD)

CD spectra were recorded on a Jasco J-810 spectropolarimeter with a Peltier system of cell temperature control. The system was routinely calibrated with an aqueous solution of twice crystallized d-10 camphorsulfonic acid. Ellipticity is reported as mean residue molar ellipticity, $[\theta]$ (deg cm^2 $dmol^{-1}$). The spectrometer conditions were typically 100 mdeg sensitivity; 0.2 nm resolution; 4 s response time; 20 nm/min scan rate, 7 accumulations at 37°C.

2.5. Protein concentration

For the CD experiments [15], protein concentrations were determined as described by Gill and von Hippel [16]. For the SDS–PAGE protein concentration were determined by the Bradford assay [17] using bovine serum albumin as standard.

3. Results

Isopropyl-β-D-thiogalactose induction of transformed DH5α *E. coli* cells triggers a time-dependent overexpression of specific proteins, the apparent molecular weight of which corresponds to the calculated mass (~110 kDa) of EP24.15 or EP24.16 fused with glutathione *S*-transferase (GST). The maximal production of the fusion proteins similarly reaches a plateau after 4 h. Proteolytic removal of GST and subsequent purification of the recombinant proteins allow the recovery of apparently homogeneous peptidases, as suggested by SDS–PAGE analysis (Fig. 1). The production yield (~0.5 mg/l of culture) was similar for all expressed proteins, suggesting that none of the mutations significantly affected the relative levels of EP24.15 or EP24.16 expression in DH5α *E. coli*.

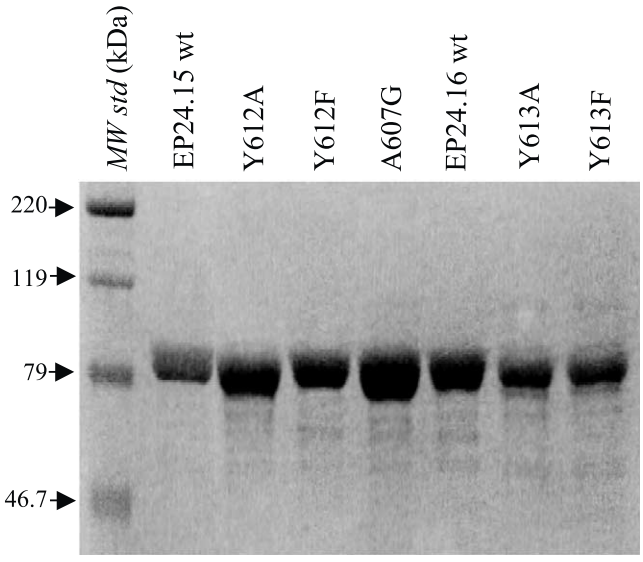

Fig. 1. SDS–PAGE of wild type and mutated EP24.15 and EP24.16. SDS–PAGE (8%) followed by Coomassie blue staining showing the homogeneity of the wild type and mutated EP24.15 and EP24.16 enzymes (15 μg each) obtained after single step affinity chromatography on a Sepharose-GST column.

In order to verify the structural integrity of the recombinant proteins, we performed far-UV CD analysis for all the enzymes produced in the present work. The obtained CD spectra for the mutants were compared with the spectra obtained for the wild type enzymes. The final CD spectra for the mutated proteins A607G, Y612F, Y612A, Y613F and Y613A were similar to that of the corresponding wild type enzyme, which shows a predominance of α-helical structure (data not shown). For the EP24.16, the results obtained from the deconvolution of the CD data, using the CDNN program [18], are consistent with the helix content observed in the enzyme crystal structure [5]. Similarly, the CD spectrum obtained for EP24.15 in the same conditions indicated 45% α-helix content, consistent with consensus secondary structure predictions obtained from different algorithms (data not shown) [19]. Moreover, we also verified similar thermal stability between the wild type and the corresponding mutant enzymes analyzed herein (data not shown).

The EP24.15 and EP24.16 mutated proteins Y612F, Y612A, Y613F and Y613A were assayed with the internally quenched fluorogenic substrate QF7 (*ortho*-aminobenzoic acid

Table 1
Comparative analyses of the kinetic constants for the hydrolysis of the Abz-GGFLRRV-EDDnp (QF7) substrate by either the wild type (WT) or mutated enzymes

Enzyme (M)		k_{cat} (s^{-1})	K_M (M)	k_{cat}/K_M (M^{-1} s^{-1})	QF7 substrate (M)
EP24.15	WT[a] (1×10^{-9})	0.70	1.7×10^{-6}	4.0×10^{5}	1×10^{-7}–1×10^{-5}
	Y612F (5×10^{-8})	5.7×10^{-3}	2.4×10^{-6}	2.4×10^{3}	1×10^{-7}–1×10^{-5}
	Y612A (3.7×10^{-7})	6.6×10^{-4}	7.1×10^{-6}	94	1×10^{-7}–2×10^{-5}
EP24.16	WT[a] (1×10^{-9})	2.0	2.2×10^{-6}	9×10^{5}	1×10^{-7}–1×10^{-5}
	Y613F (4.2×10^{-8})	7.8×10^{-3}	1.2×10^{-6}	6.5×10^{3}	1×10^{-7}–1×10^{-5}
	Y613A (3.4×10^{-7})	2.5×10^{-4}	2.8×10^{-6}	89	1×10^{-7}–1×10^{-5}

[a]Our previously published results [22]. The QF7 substrate was hydrolyzed at the Leu-Arg peptide bond.

Table 2
Comparative kinetic constants for the hydrolysis of substrates Abz-GFSIFRQ-EDDnp and Abz-GGFLRRV-EDDnp (QF7) by wild type (WT) EP24.15 or its A607G mutant

Substrate	EP24.15 (M)	k_{cat} (s^{-1})	K_M (M)	k_{cat}/K_M (M^{-1} s^{-1})	Substrates (M)
Abz-GGFL↓RRV-EDDnp (QF7)	WT[a] (1×10^{-9})	0.70	1.7×10^{-6}	40×10^{4}	1×10^{-7}–1×10^{-5}
	A607G (1×10^{-10})	3.1	4.4×10^{-6}	70×10^{4}	1×10^{-7}–1.5×10^{-5}
Abz-GFSI↓FRQ-EDDnp	WT (5×10^{-8})	0.010	0.4×10^{-6}	2.5×10^{4}	1×10^{-7}–5×10^{-6}
	A607G (7×10^{-9})	0.099	0.5×10^{-6}	2×10^{5}	1×10^{-7}–5×10^{-6}

[a]Our previously published results [22].

(Abz)-GGFLRRV-*N*-(2,4-dinitrophenyl) ethylenediamine (EDDnp)) in order to compare their hydrolytic activity with that of the wild type enzymes. k_{cat}/K_M reductions of 138- and 10 112-fold for the EP24.16 mutants Y613F and Y613A, respectively, were observed in comparison to the wild type enzyme (Table 1). Similarly, the EP24.15 mutants Y612F and Y612A hydrolyzed the QF7 substrate 167- and 4255-fold, respectively, less efficiently than the wild type enzyme (Table 1). These differences in the k_{cat}/K_M ratio were mainly due to a reduction of k_{cat} (Table 1). However, for the EP24.15 Y612A mutant a four-fold increase in the K_M (7.1×10^{-6} M) compared to the wild type EP24.15 (1.7×10^{-6} M) was observed (Table 1).

The EP24.15 mutant A607G was assayed with both QF7 and Abz-GFSIFRQ-EDDnp substrates. We have previously reported that the peptide Abz-GFSIFRQ-EDDnp was a better competitive inhibitor than substrate for the EP24.15, using an enzyme concentration up to 1×10^{-8} M [6,22]. In the present work, we increased the EP24.15 enzyme concentration five-fold to obtain the kinetic parameters for the Abz-GFSIFRQ-EDDnp substrate (Table 2). The A607G mutant, like the wild type EP24.15, hydrolyzed this substrate at the Ile-Phe bond (Table 2). However, the A607G mutant shows a k_{cat} 10 times higher than wild type EP24.15, with no significant changes in the K_M values (Table 2). The k_{cat}/K_M value obtained for the EP24.15 A607G mutant (2×10^{5} M^{-1} s^{-1}; Table 2) is similar to that previously described for the wild type EP24.16 (3×10^{5} M^{-1} s^{-1}) [6].

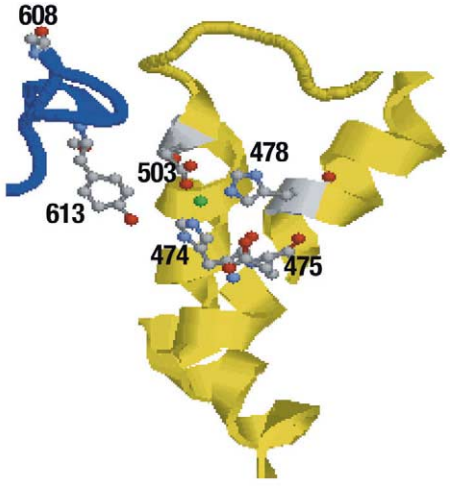

Fig. 2. Details of the EP24.16 active site region. The nearby disordered loop shown in blue corresponds to residues 600–612. The Tyr^{613} residue was the one mutated to either Phe or Ala. Gly^{608} from EP24.16 corresponds to Ala^{607} on EP24.15, which was mutated herein to Gly (A607G). The green sphere represents the catalytic zinc ion.

4. Discussion

A major finding of our present study is the demonstration that a specific Tyr residue in the vicinity of the catalytic site of both EP2415 and EP24.16 actively participates in peptide substrate hydrolysis. We have also shown here that Ala^{607} plays an important role in EP24.15 substrate specificity.

The Tyr^{613} residue on EP24.16 is close to the catalytic zinc ion from the active site (Fig. 2), similarly to Tyr^{612} in the EP24.15 [5,9]. Such proximity to the active center suggested this residue is in a position to contribute to the catalytic mechanism of EP24.16 and EP24.15, as previously suggested for Tyr^{157} from thermolysin [20] or Tyr^{149} from astacin [21]. However, different from thermolysin, a nearby His residue (His^{231} in thermolysin) is absent in both the EP24.15 and EP24.16 active centers [5]. In this context, the catalytic mechanism of EP24.16 and EP24.15 may be more related to that of astacin. In astacin, Tyr^{149} is thought to be important both for substrate binding and for transition state stabilization [21]. Thus, we are showing for the first time that a specific amino acid residue outside the zinc binding HEXXH+E motif is directly involved in substrate hydrolysis by both EP24.15 and EP24.16. Similarly to what occurs in astacin and also in thermolysin, in EP24.15 and EP24.16 the hydroxyl group from this Tyr could be important to stabilize the oxyanion intermediate formed after nucleophilic attack by the water molecule [20,21].

Interestingly, there are differences in the mutants in which the Tyr residue was replaced by Phe, compared to the ones where the same Tyr residue was replaced by Ala. Substitution of Tyr^{612} (EP24.15) or Tyr^{613} (EP24.16) by Phe reduced by two orders of magnitude the degradation of the fluorogenic QF7 substrate. However, substitution of this Tyr by Ala, on both enzymes, reduced hydrolysis of the QF7 substrate by up to four orders of magnitude (Table 1). Therefore, it seems that both the hydroxyl group and the aromatic ring of this Tyr are important for substrate catalysis by both EP24.15 and EP24.16. The corresponding Tyr residue is conserved among the peptidases belonging to the M3 family of metallopeptidases, including oligopeptidase F from *Lactococcus lactis* [23]. Interestingly, no enzymatic activity has been reported for the oligopeptidase F from *Listeria monocytogenes* and from *Listeria innocua* and four other unassigned peptidases from the M3 family that have a Phe residue in the place of this Tyr residue [23]. Altogether, these observations suggest that this amino acid residue could be important for the catalytic mechanism of other members of the M3 family of metallopeptidases.

It has been suggested that the broad substrate specificity of this enzyme can be attributed to the fact that the substrate binding region of this peptidase is lined with flexible loops [5]. Among these potential substrate binding regions of EP24.16 it

is interesting to note the presence of a loop composed of residues 600–612 (Fig. 2). This region presents a high average temperature factor, and the high content of Gly residues (five in 12 residues) is thought to contribute to the flexibility of this portion of EP24.16 [5,9]. Furthermore, this loop is the most probable portion of the enzyme to interact with the amino acid residue located at the P_1 position of the peptide substrates. This suggestion has been corroborated by modeling of a substrate molecule of neurotensin in the EP24.16 active site [5]. One of the major differences found in the specificity of these enzymes was the better acceptance by EP24.16 of substrates containing Ile at the P_1 position [6]. The unique difference found in this loop for these two peptidases is the presence of Ala^{607} on EP24.15 in the place of Gly^{608} on EP24.16. We then produced an EP24.15 mutant (A607G) that hydrolyzed peptide Abz-GFSIFRQ-EDDnp at the Ile–Phe bond (Ile residue at the P_1 position), more efficiently than wild type EP24.15 (Table 2), and with k_{cat}/K_M similar to that of wild type EP24.16 [6]. These data suggest that Ala^{607} is an important residue to drive the substrate specificity of EP24.15, probably by direct interaction with the substrate or by changing the flexibility of the loop, which is in a position to interact with the P_1 residue of the substrate [5,9]. In addition, the modeling of a substrate (neurotensin) in the active site of EP24.16 indicates Tyr^{606} (conserved in the EP24.15 sequence) as the most probable residue that interacts with the P_1 side chain of the substrate [5]. It is interesting that the constant that could represent the enzyme affinity by the substrate remained the same for either the wild type EP24.15 ($K_M = K_i = 0.4\times10^{-6}$ M) or the A607G mutant ($K_M = 0.5\times10^{-6}$ M) (Table 2). It means that the accommodation of the P_1 substrate residue corresponds more to a catalytic step, possibly through a structural rearrangement of the substrate binding region in the enzyme that does not account for the K_M constant. Moreover, a high and positive entropy of activation has been described for the hydrolysis of the QF7 and related substrates by both EP24.15 and EP24.16 [22], which can be interpreted as a structural rearrangement during the catalysis of peptide substrates by these two peptidases.

In conclusion, the present report has demonstrated the participation of specific amino acid residues in the specificity and catalytic mechanism of both EP24.15 and EP24.16.

Acknowledgements: This work was supported by the Fundação de Amparo a Pesquisa do Estado de São Paulo (FAPESP) through Structural Biology Network Program (Smolbnet) Grant 01/07544-9. E.S.F., I.T., A.C.M.C. and L.J. acknowledge the Brazilian National Research Council – CNPq for research fellowships. V.O., M.C.A. and V.R. are fellowship recipients from FAPESP.

References

[1] Orlowski, M., Michaud, C. and Chu, T.G. (1983) Eur. J. Biochem. 135, 81–88.
[2] Checler, F., Vincent, J.P. and Kitagib, P.J. (1986) J. Biol. Chem. 261, 11274–11281.
[3] Pierotti, A., Dong, K., Glucksman, M.J., Orlowski, M. and Roberts, J.L. (1990) Biochemistry 29, 10323–10329.
[4] Dauch, P., Vincent, J.P. and Checler, F. (1995) J. Biol. Chem. 270, 27266–27271.
[5] Brown, C.K., Madauss, K., Lian, W., Beck, M.R., Tolbert, W.D. and Rodgers, D.W. (2001) Proc. Natl. Acad. Sci. USA 98 (6), 3127–3132.
[6] Oliveira, V., Campos, M., Melo, R.L., Ferro, E.S., Camargo, A.C.M., Juliano, M.A. and Juliano, L. (2001) Biochemistry 40 (14), 4417–4425.
[7] Barrett, A.J. and Rawlings, N.D. (1992) Biol. Chem. Hoppe-Seyler 373, 353–360.
[8] Camargo, A.C.M., Caldo, H. and Reis, M.L. (1979) J. Biol. Chem. 254, 5304–5307.
[9] Ray, K., Hines, C.S. and Rodgers, D.W. (2002) Protein Sci. 119 (9), 2237–2246.
[10] Oliveira, V., Campos, M., Hemerly, J.P., Ferro, E.S., Camargo, A.C.M., Juliano, M.A. and Juliano, L. (2001) Anal. Biochem. 292, 257–265.
[11] Rioli, V., Gozzo, F.C., Heimann, A.S., Linardi, A., Krieger, J.E., Shida, C.S., Almeida, P.C., Hyslop, S., Eberlin, M.N. and Ferro, E.S. (2003) J. Biol. Chem. 278, 8547–8555.
[12] Rioli, V., Kato, A., Portaro, F.C.V., Cury, G.K., Te Kaat, K., Vincent, B., Checler, F., Camargo, A.C.M., Glucksman, M.J., Roberts, J.L., Hirose, S. and Ferro, E.S. (1998) Biochem. Biophys. Res. Commun. 250, 5–11.
[13] Araújo, M.C., Melo, R.L., Cesari, M.H., Juliano, M.A., Juliano, L. and Carmona, A.K. (2000) Biochemistry 39, 8519–8525.
[14] Wilkinson, G.N. (1961) Biochem. J. 80, 324–332.
[15] Altschul, S.F., Madden, T.L., Schäffer, A.A., Zhang, J., Zhang, Z., Miller, W. and Lipman, D.J. (1997) Nucleic Acids Res. 25, 3389–3402.
[16] Gill, S.C. and von Hippel, P.H. (1989) Anal. Biochem. 182, 319–326.
[17] Bradford, M.M. (1976) Anal. Biochem. 72, 248–254.
[18] Böhm, G. (1997) CDNN-CD Spectra Deconvolution Version 2.1, ACGT ProGenomics AG, Halle (Saale).
[19] Combet, C., Blanchet, C., Geourjon, C. and Deléage, G. (2000) Trends Biochem. Sci. 25, 147–150.
[20] Marie-Claire, C., Ruffet, E., Tiraboschi, G. and Fournie-Zaluski, M.C. (1998) FEBS Lett. 438, 215–219.
[21] Yiallouros, I., Berkhoff, E.G. and Stocker, W. (2000) FEBS Lett. 484, 224–228.
[22] Oliveira, V., Gatti, R., Rioli, V., Ferro, E.S., Spisni, A., Camargo, A.C.M., Juliano, M. and Juliano, L. (2002) Eur. J. Biochem. 269, 4326–4334.
[23] Rawlings, N.D. and Barrett, A.J. (2000) Nucleic Acids Res. 33, 323–325.